Molecular Biology of the Cell
Vol. 21, 302–310, January 15, 2010

Caveolin-3 Promotes Nicotinic Acetylcholine Receptor Clustering and Regulates Neuromuscular Junction Activity

Michael Hezel, William C. de Groat, and Ferruccio Galbiati

Department of Pharmacology and Chemical Biology, University of Pittsburgh School of Medicine, Pittsburgh, PA 15261

Submitted May 8, 2009; Revised October 29, 2009; Accepted November 17, 2009
Monitoring Editor: Carl-Henrik Heldin

The molecular mechanisms that regulate the organization and activity of the neuromuscular junction remain to be fully identified. Caveolae are invaginations of the plasma membrane. Caveolin-3 is the structural protein component of caveolae in muscle cells. We show that caveolin-3 is expressed at the neuromuscular junction, that it associates with the nicotinic acetylcholine receptor (nAChR), and that a lack of caveolin-3 inhibits clustering of the nAChR in myotubes. At the molecular level, we demonstrate that caveolin-3 is a novel muscle-specific kinase (MuSK) binding protein and that altered nAChR clustering in caveolin-3–lacking myotubes results from inhibition of agrin-induced phosphorylation/activation of MuSK and activation of Rac-1. Functional studies in caveolin-3 null mice show abnormal neuromuscular junction activity that is consistent with altered nAChR localization at the sarcolemma. Together, these data identify caveolin-3 as a critical component of the signaling machinery that drives nicotinic acetylcholine receptor clustering and controls neuromuscular junction function.

INTRODUCTION

Proper organization of the neuromuscular junction (NMJ) is important for efficient and effective movement. The formation of the neuromuscular junction is a complex process. At mouse embryonic day 14, the nerve starts to innervate the muscle and releases the neuronal peptide agrin (Sanes and Lichtman, 2001). On its release, neural agrin crosses the synapse and associates with muscle-specific kinase (MuSK), a transmembrane receptor tyrosine kinase (Ferns *et al*., 1993). MuSK then undergoes autophosphorylation, initiating a phosphorylation cascade that induces the nicotinic acetylcholine receptor (nAChR) to concentrate in the muscle directly across from the nerve terminal. After birth, the NMJ is further refined to one nerve terminal per myotube and the muscle membrane forms folds at the NMJ with the nAChR located at the crests directly juxtaposed to the nerve terminal (Sanes and Lichtman, 2001). This proximity of the nerve and nAChR on the muscle is essential for rapid contractile signaling.

The nAChR is a heteropentameric ligand-gated ion channel located at the muscle membrane. In the muscle, the nAChR consists of two α subunits involved in ligand binding, one β subunit, one δ subunit, and one γ subunit. During postnatal modification of the NMJ, nAChR with the γ subunit are replaced with nAChR containing the ε subunit. The ε subunit adds stability to the receptor, thereby increasing the half-life of the receptor (Sanes and Lichtman, 2001).

Caveolae, 50- to 100-nm flask-shaped invaginations of the plasma membrane, are found in many cell types, but they are particularly abundant in fibroblasts, adipocytes, endothelial cells, type I pneumocytes, epithelial cells, and smooth/striated muscle cells (Razani *et al*., 2000; Hagiwara *et al*., 2002; Volonte *et al*., 2003). Caveolae represent a subgroup of lipid rafts, which are microdomains of the plasma membrane enriched in cholesterol, sphingolipids, and glycosyl phosphatidylinositol-anchored proteins (Razani *et al*., 2000). The presence of the structural protein caveolin (Cav) drives the formation of the plasma membrane invaginations and makes caveolae unique among lipid rafts. Caveolae have been implicated in numerous cellular functions, including signal transduction, cellular metabolism, vesicle trafficking, cholesterol homeostasis, endothelial transcytosis, and tumor suppression (Razani *et al*., 2000; Hagiwara *et al*., 2002; Williams and Lisanti, 2004).

There are three isoforms of caveolin: caveolin-1, -2, and -3. They are highly conserved across species and have molecular masses averaging 18–24 kDa (Razani *et al*., 2000; Williams and Lisanti, 2004). Caveolin-1 and -2 are mapped to the 7q31.1 human chromosome, and caveolin-3 is found on 3p25 (Razani *et al*., 2000; Williams and Lisanti, 2004). Caveolins act as scaffolding proteins to compartmentalize and functionally regulate signaling molecules within caveolar membranes (Razani *et al*., 2000).

Based on protein sequence homology, caveolin-3 is most closely related to caveolin-1: caveolin-1 and caveolin-3 are ~65% identical and ~85% similar (Tang *et al*., 1996). However, caveolin-3 mRNA and protein are expressed predominantly in muscle tissue types (skeletal muscle, diaphragm, and heart) (Moldovan *et al*., 1995; Aravamudan *et al*., 2003; Volonte *et al*., 2003, 2008). Identification of a muscle-specific member of the caveolin gene family has implications for understanding the role of caveolins in different muscle cell types (smooth, cardiac, and skeletal), as previous morphological studies have demonstrated that caveolae are abundant in these cells. In muscle cells, the presence of caveolin-3 is sufficient to produce caveolae at the membrane (Li *et al*., 1998). In differentiated skeletal muscle cells in vitro, and myotubes in vivo, caveolin-3 is mainly associated with the sarcolemma, where it acts as a scaffolding protein that con-

This article was published online ahead of print in *MBC in Press* (http://www.molbiolcell.org/cgi/doi/10.1091/mbc.E09–05–0381) on November 25, 2009.

Address correspondence to: Ferruccio Galbiati (feg5@pitt.edu).

centrates and functionally regulates signaling molecules (Volonte *et al*., 2003; Hezel *et al*., 2005). The role of caveolin-3 as a potential regulator of the organization and function of the neuromuscular junction remains to be elucidated.

Here, we show that caveolin-3 promotes agrin-induced clustering of the nAChR in skeletal muscle cells through activation of the MuSK/Rac-1 pathway and modulates neuromuscular junction function.

MATERIALS AND METHODS

Materials

Antibodies and their sources were as follows: anti-acetylcholine receptor α immunoglobulin (Ig)Gs (monoclonal antibody [mAb] clone 26), anti-caveolin-3 IgGs (mAb clone 26), and anti-phosphotyrosine (mAb clone PY20) were purchased from BD Biosciences Transduction Laboratories (San Jose, CA). Anti-caveolin-3 IgGs (pAb N-18) and anti-MuSK IgGs (pAb C-19) were from Santa Cruz Biotechnology (Santa Cruz, CA). Anti-MuSK (pAb PA1-1740) and anti-Rac1 IgGs (mAb clone 23A8) were from Affinity BioReagents (Golden, CO). Anti-MuSK (mAb) was a generous gift from Dr. Steven Burden (New York University School of Medicine, New York, NY). Anti-nicotinic acetylcholine receptor IgGs (mAb clone 35) and anti-β-tubulin 3 IgGs (mAb TUJ1) were from Covance (Berkeley, CA). Anti-phosphotyrosine IgGs (mAb clone 4G10) was from Millipore Bioscience Research Reagents (Temecula, CA). The glutathione transferase (GST)-p21-binding domain (PBD) construct was kindly provided by Dr. Daniel Altschuler (Department of Pharmacology and Chemical Biology, University of Pittsburgh, Pittsburgh, PA). All chemicals were of the highest purity available and purchased from either Sigma-Aldrich (St. Louis, MO) or Thermo Fisher Scientific (Waltham, MA).

Cell Culture

Conditionally immortalized wild-type and caveolin-3 knockout myoblasts were obtained as described previously (Volonte *et al*., 2003). Myoblasts were grown at 33°C using proliferation media: Ham's F-10 containing 20% fetal bovine serum, 2 mM L-glutamine, 100 units/ml penicillin, 100 μg/ml streptomycin, basic fibroblast growth factor (2.5 ng/ml), and γ-interferon (50 U/ml). Differentiation from myoblasts (90% confluence) to myotubes was achieved by culturing the cells at 37°C for 7 d in differentiation media: DMEM containing 2% horse serum, 2 mM L-glutamine, 100 U/ml penicillin, and 100 μg/ml streptomycin. To induce acetylcholine receptor clustering, 10 ng/ml rat agrin (R&D Systems, Minneapolis, MN) was added to the differentiation media. H-Ras (G12V)-expressing cells were grown in DMEM with 10% donor bovine serum, 2 mM L-glutamine, 100 U/ml penicillin, and 100 μg/ml streptomycin.

Immunofluorescence Staining

Tissue Sections. Quadriceps or gastrocnemius tissues from wild-type and caveolin-3 null mice were dissected, embedded in OCT embedding medium, and rapidly frozen in liquid nitrogen-cooled isopentane. Cross-sections (5 μm in thickness) were incubated with monoclonal mouse anti-nAChR-α and polyclonal goat anti-caveolin-3 antibodies (diluted 1:500 in phosphate buffered solution with calcium and magnesium [PBS-CM] containing 0.1% Triton X-100 [PBS-CM-T]) at room temperature for 3 h. Slides were washed three times (10 min each) in PBS-CM-T. Slides were then incubated for 2 h in secondary antibodies (1:1000 dilution in PBS-CM-T). Slides were washed three times in PBS-CM-T for 10 min each, and a coverslip was mounted on the tissue with slow-Fade antifade reagent (Invitrogen, Carlsbad, CA) and sealed with nail polish.

Whole-Mount Staining. The extensor digitorum longus (EDL) muscle was fixed in 2% paraformaldehyde in 0.1% phosphate buffered solution, pH 7.3, overnight at 4°C. The tissue was rinsed in PBS, pH 7.3, and incubated in 0.1 M glycine in PBS for 1 h. The tissue was rinsed again in PBS and incubated in 0.5% Triton X-100 solution in PBS for 1 h. The muscle was blocked in dilution buffer (500 mM NaCl, 0.01 M phosphate buffer, and 0.01% thimerosal) overnight at 4°C. The tissue was then incubated with primary antibodies (Cav-3, 1:500; β-tubulin 3, 1:500) in dilution buffer overnight at 4°C. The tissue was rinsed three times with 0.5% Triton X-100 in PBS (1 h each wash) and incubated with fluorescent secondary antibodies (1:1000) and α-bungarotoxin (α-Btx, 1:500) in dilution buffer and incubated overnight at 4°C. The tissue was then washed three times in 0.5% Triton X-100 solution in PBS (1 h each wash). The tissues were rinsed once in PBS, mounted on a slide with antifade solution, and analyzed by confocal microscopy.

Cells on Coverslips. Cells were grown on coverslips and treated as required for the experiment. At the time of staining, the cells were washed three times in PBS-CM and fixed with 2% paraformaldehyde in PBS solution for 30 min. Cells were made permeable with PBS-CM-T for 10 min and peroxides quenched with ammonium chloride in PBS-CM for 10 min followed by a rinse with PBS-CM-T. Incubation with primary and secondary antibodies was then performed as described above with tissue sections.

nAChR Analysis

Wild-type and caveolin-3 knockout myogenic precursor cells were grown on coverslips, differentiated for 7 d, and treated with agrin for 24 h. The cells were stained for caveolin-3 and nAChR by using specific antibody probes. The cells were analyzed by confocal microscopy, pictures were taken, and the lengths and the number of clusters per field were measured.

DNA Constructs

Using mRNA from skeletal muscle cells, wild-type MuSK cDNA was amplified by reverse transcription-polymerase chain reaction (PCR) by using the following primers: 5′, ccg gcc gtc gac aag aga gct cgt caa cat tcca; and 3′, cc ggc cgc ggc cgc tta gac act cac agt tcc ctc. MuSK cDNA was then digested with SalI and NotI and cloned into the pCMV-hemagglutinin (HA) expression vector. The following two MuSK constructs with mutated caveolin binding domains were generated: 1) replacement of amino acids W786, Y788, and W793 with alanines; and 2) replacement of amino acids F796, Y798, Y803, and Y804 with alanines. Both MuSK mutants were generated by PCR amplification using appropriate internal primers and subcloned into the pCMV-HA vector.

Western Blotting Analysis

Samples analyzed by Western blotting were boiled for 5 min after addition of Laemmli buffer and loaded into a 12.5% Tris-HCl polyacrylamide gel. The gel was run at 40 mAmps per gel and transferred to nitrocellulose membranes overnight at 4°C at 150 mAmps per gel. The nitrocellulose was blocked in 2% milk in Tris-buffered saline with Tween 20 (TBST) for monoclonal antibodies or in 2% milk, 1% bovine serum albumin in TBST for polyclonal antibodies. The membrane was washed with TBST and incubated overnight with the primary antibody. The next day, the blot was washed with TBST and then incubated with the secondary antibody in blocking solution. The blot was washed again with TBST and then developed using SuperSignal solution (Pierce Chemical, Rockford, IL), and results were captured on Kodak X-Omat film (PerkinElmer Life and Analytical Sciences, Boston, MA).

Immunoprecipitation

Cells were washed in PBS, collected, and resuspended in lysis buffer (10 mM Tris-HCl, pH 8.0, 150 mM NaCl, 5 mM EDTA, 1% Triton X-100, 60 mM *n*-octyl glucoside, and protease inhibitors). Tissue was placed in lysis buffer and underwent mechanical homogenization using a Tissue-Tearor (BioSpec Products, Bartlesville, OK) for 30 s. Samples were put on rotation at 4°C for 1 h. The insoluble material was precipitated by centifugation, and the supernatant was collected. The samples were precleared with 10 μl of protein A-Sepharose slurry (beads:lysis buffer, 1:1), and then protein content was measured by bicinchoninic acid assay (Promega). Samples were normalized to have the same protein content and volume. Antibody and protein A-Sepharose beads were then added to the samples. Samples were put on rotation overnight at 4°C. Beads were washed three times with lysis buffer and once with 50 mM Tris-HCl. Beads were resuspended in Laemmli buffer, boiled, and centrifuged, and the supernatant was subjected to immunoblotting analysis.

Fusion of GST-PBD to Agarose Beads

GST constructs in BL21 bacteria were grown at 37°C in ampicillin containing Luria broth to an optical density between 0.3 and 0.6. Isopropyl β-D-thiogalactoside was added to achieve a final concentration of 0.5 mM, and samples were left shaking at 37°C for 2 h. Bacteria were centrifuged and washed in 150 mM NaCl, 7.5 mM Tris, pH 8.0, and 3 mM EDTA (STE) and resuspended in 10 ml of STE. Then, 10 μg/ml lysozyme was added to the bacterial solution, and samples were incubated on ice for 15 min. We added 5 mM dithiothreitol, 1.5% *n*-lauryl sarkosyl, and protease inhibitors to the samples. Cells were homogenized using a Tissue-Tearor at medium speed for 30 s and centrifuged for 20 min to remove insoluble material. The supernatant was taken, and 2% Triton X-100 was added to the samples. Glutathione bound to agarose beads was then added, and samples were incubated on rotation overnight at 4°C. The beads were washed three times in STE with 1% Triton X-100 and incubated with cell lysates as described below for GST-PBD pulldown.

GST-PBD Pulldown

Cells were washed, collected, and resuspended in lysis buffer consisting of 50 mM Tris-HCl, 0.5% sodium deoxycholate, 0.1% SDS, 150 mM sodium chloride, 10 mM magnesium chloride, 1% Triton, and protease inhibitors. Cells were put on rotation for 1 h at 4°C. Insoluble material was precipitated, and the supernatant was collected. The samples were precleared with unbound glutathione-conjugated agarose beads. Samples were normalized to have the same protein content and volume. GST-PBD–bound glutathione beads were then added to each sample and put on rotation overnight at 4°C. The beads were washed three times with lysis buffer without SDS and sodium deoxycholate. Laemmli buffer was added to the beads, which were vortexed, boiled

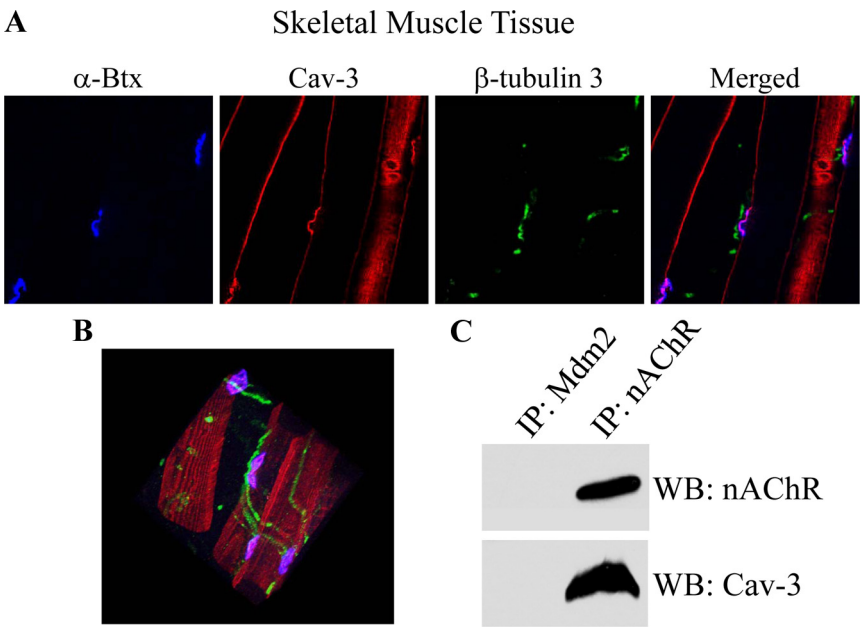

Figure 1. Caveolin-3 and nAChR localization and association in skeletal muscle tissue. (A) Whole-mount EDL muscles from wild-type mice were stained for Cav-3 (red), α-Btx (blue), and β-tubulin 3 (green) expressions. Representative confocal images are shown. (B) 3D reconstruction of the staining is shown. A representative video can be found in Supplemental Data. (C) Gastrocnemius muscles were derived from wild-type C57Bl6 mice. Muscle cell lysates were then subjected to immunoprecipitation with a mAb specific for the α subunit of the nAChR (mAb 35) and immunoprecipitates subjected to immunoblotting analysis with monoclonal antibodies specific for caveolin-3 (mAb 26; Cav-3) and the α subunit of the nAChR (mAb 26; nAChR). Immunoprecipitation with a mAb probe specific for the oncoprotein Mdm2 was used as internal control to demonstrate specificity.

for 5 min, and centrifuged at 13,000 rpm for 5 min. The supernatant was then subjected to immunoblotting analysis.

Electromyography (EMG) and Muscle Contraction Experiments

Wild-type and caveolin-3 null mice were anesthetized by intraperitoneal injection of urethane (1.2 mg/kg). A tracheotomy was performed using 1.57-mm-diameter tubing to facilitate respiration. The Achilles tendon was exposed, tied to a force displacement transducer (FT-10; Grass Technologies, West Warwick, RI), and cut proximal to the ankle. The sciatic nerve to the ipsolateral side was exposed, and skin flaps were tied up forming a pool. The pool was filled with mineral oil to insulate and prevent drying of the sciatic nerve. A 0.25-mm bipolar silver stimulating electrode was placed on the nerve 1 cm away from the muscle. The nerve was cut centrally to eliminate reflex responses. A recording electrode (SNE-100; Rhodes Medical Instruments, Summerland, CA) was placed into the middle of the gastrocnemius muscle through a small incision in the skin covering the gastrocnemius muscle. The nerve was stimulated with a range of intensities (0.05-ms pulse duration) to determine the intensities necessary to elicit threshold and maximal responses. A varying range of stimulus frequencies (1, 10, and 50 Hertz) was also examined. Compound muscle action potentials (CMAP) and muscle contractile force responses by evoked supramaximal sciatic nerve stimulation were collected simultaneously. Various data were analyzed using LabVIEW 7.0 (National Instruments, Austin, TX), including latency, peak-to-peak amplitude, and area under the curve (AUC) of CMAP as well as amplitude and pattern of evoked muscle contractions.

RESULTS

Caveolin-3 Is Enriched at the Neuromuscular Junction and Associates with the nAChR in Skeletal Muscle Tissue

To investigate whether caveolin-3 plays a role in neuromuscular junction signaling, we first examined whether caveolin-3 was localized at the neuromuscular junction in mouse skeletal muscle tissue by immunofluorescence staining. We show that caveolin-3 is expressed in skeletal muscle tissue and is enriched at the neuromuscular junction (NMJ), as demonstrated by staining with anti-caveolin-3 IgGs and α-Btx (Figure 1A) or anti-caveolin-3 IgGs and an antibody probe specific for the α subunit of the nAChR (Supplemental Figure 1, A and B). The three-dimensional (3D) image in Figure 1B confirms enrichment of caveolin-3 at the neuromuscular junction (see Supplemental Data for a representative video). We also demonstrate in Figure 1, A and B, that caveolin-3 is not expressed at the nerve terminal, as shown by lack of colocalization between caveolin-3 and β-tubulin 3, a neuron-specific marker. The association of nAChR with caveolin-3 was further bolstered by the coimmunoprecipitation of caveolin-3 and nAChR-α in skeletal muscle tissue homogenates (Figure 1C).

Agrin Promotes Association between nAChR and Caveolin-3 in Cultured Myotubes

To investigate whether the in vivo results could be replicated in cell culture models, myoblasts derived from wild-type mice were differentiated for 7 d into myotubes and treated with neural agrin for 24 h to induce nAChR clustering. Treatment with neural agrin is a well-established way to induce muscle nAChR clustering in the absence of innervation. Myotubes were double stained with anti-caveolin-3 and anti-nAChR-α IgGs. Consistent with Figure 1 data, caveolin-3 was expressed throughout the sarcolemma but was enriched in discrete areas of the plasma membrane expressing the nAChR (Figure 2A). To confirm that actual association occurs between caveolin-3 and the nAChR in skeletal muscle cells, we immunoprecipitated the nAChR from differentiated myotubes treated with and without agrin by using α-Btx. Figure 2B shows that caveolin-3 coimmunoprecipitated with the nAChR and that agrin treatment for 24 h increased their association. Quantitatively, 0.01% caveolin-3 associated with 4% nAChR that was precipitated before agrin treatment, whereas 0.2% caveolin-3 associated with 4% nAChR that was precipitated after agrin treatment; thus, 0.25% caveolin-3 interacts with the nAChR under resting conditions; 5% caveolin-3 interacts with the nAChR after agrin treatment. These results are consistent with the immunofluorescence data in Figures 1, A and B, and 2B, showing that caveolin-3 is only partially localized in nAChR-expressing areas of the sarcolemma. Together, these data indicate that caveolin-3 is indeed expressed at the neuromuscular junction in skeletal muscle cells and that agrin promotes its interaction with the nAChR by ~20-fold.

To estimate the relative stoichiometry of caveolin-3 and nAChR, we transiently expressed myc-tagged versions of both caveolin-3 and nAChR-α at a ratio of 1:3, so that all cells

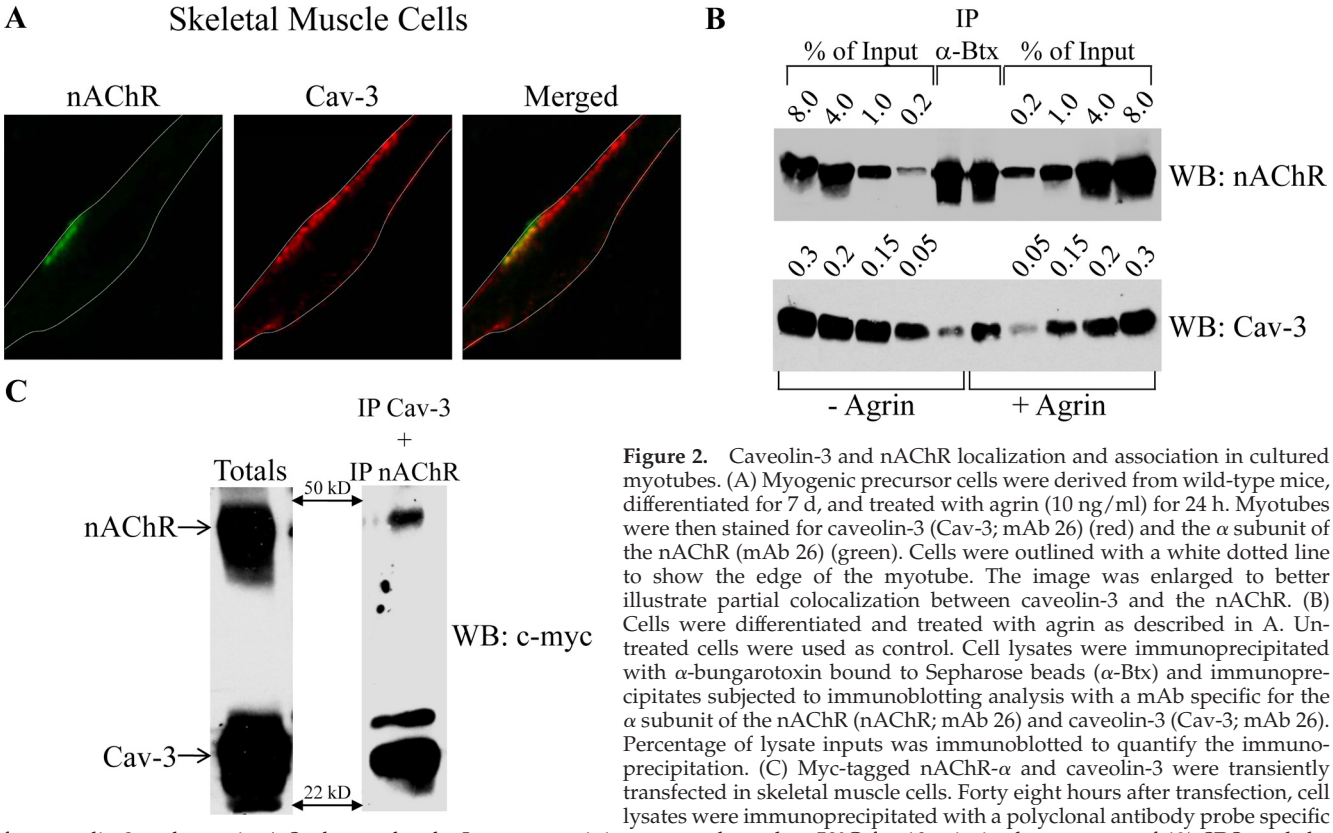

Figure 2. Caveolin-3 and nAChR localization and association in cultured myotubes. (A) Myogenic precursor cells were derived from wild-type mice, differentiated for 7 d, and treated with agrin (10 ng/ml) for 24 h. Myotubes were then stained for caveolin-3 (Cav-3; mAb 26) (red) and the α subunit of the nAChR (mAb 26) (green). Cells were outlined with a white dotted line to show the edge of the myotube. The image was enlarged to better illustrate partial colocalization between caveolin-3 and the nAChR. (B) Cells were differentiated and treated with agrin as described in A. Untreated cells were used as control. Cell lysates were immunoprecipitated with α-bungarotoxin bound to Sepharose beads (α-Btx) and immunoprecipitates subjected to immunoblotting analysis with a mAb specific for the α subunit of the nAChR (nAChR; mAb 26) and caveolin-3 (Cav-3; mAb 26). Percentage of lysate inputs was immunoblotted to quantify the immunoprecipitation. (C) Myc-tagged nAChR-α and caveolin-3 were transiently transfected in skeletal muscle cells. Forty eight hours after transfection, cell lysates were immunoprecipitated with a polyclonal antibody probe specific for caveolin-3 and protein A-Sepharose beads. Immunoprecipitates were heated at 50°C for 10 min in the presence of 1% SDS, and the supernatant subjected to a second round of immunoprecipitation with a mAb probe specific for nAChR-α (mAb 26). Immunoprecipitates were then subjected to immunoblotting analysis with an anti-c-myc mAb. Total expression of nAChR-α-myc and caveolin-3-myc are shown in the left panel.

expressing caveolin-3 should express nAChR. Cell lysates were subjected to sequential immunoprecipitation with a polyclonal antibody probe specific for caveolin-3 followed by a mAb probe specific for the nAChR-α. Immunoprecipitates were then subjected to immunoblotting analysis by using anti-myc IgGs to detect both caveolin-3-c-myc and nAChR-α-c-myc. Quantitative immunoblotting determined the ratio of caveolin-3 to nAChR to be ~14 (Figure 2C). Because caveolin-3 forms homo-oligomers containing ~14–16 caveolin monomers per oligomer (Tang *et al*., 1996), it is possible that each caveolin-3 oligomeric complex may contain one molecule of α-nAChR.

Caveolin-3 Expression Promotes nAChR Clustering

We then asked whether caveolin-3 plays a role in the clustering of the nAChR. To this end, myogenic precursor cells were derived from wild-type and caveolin-3 null mice, which do not express caveolin-3, and differentiated to myotubes. In agrin-untreated myotubes, minimal clustering of the nAChR was observed in both wild-type and caveolin-3 null myotubes (Figure 3A). After treatment with agrin, we found that clustering of nAChR was defective in caveolin-3 null myotubes, as shown by a more diffuse staining along the sarcolemma compared with wild-type myotubes, in which the nAChR seemed more concentrated in discrete areas (Figure 3B). Quantification of cluster length shows that nAChR clusters in agrin-treated caveolin-3 null myotubes were ~50% longer than clusters found in caveolin-3–expressing myotubes (Figure 3C). Consistent with these data, lack of caveolin-3 resulted in an ~60% reduction in the number of clusters per field after agrin treatment (Figure 3D).

Caveolin-3 Is a Novel MuSK-binding Protein

Local release of agrin by the nerve and the consequent activation of MuSK in skeletal muscle cells initiate a signaling cascade that leads to clustering of the nAChR. Because our data indicate that caveolin-3 expression promotes nAChR clustering, we asked whether caveolin-3 plays a role in MuSK function. Caveolins have been shown to directly bind to signaling proteins carrying one or more of the following sequences ΦXΦXXXXΦ, ΦXXXXΦXXΦ, or ΦXΦXXXXΦXXΦ (where Φ represents the aromatic amino acids phenylalanine, tyrosine, and tryptophan and X represents any other amino acid; Couet *et al*., 1997b). Analysis of the MuSK protein sequence shows that it contains two putative caveolin binding domains (CBDs) located in the kinase domain of the cytoplasmic region (CBD-A, ^{786}WaYgvvlW^{793}; CBD-B, ^{796}FsYglqpY^{803}; Supplemental Figure 2A). To directly prove that these two sequences represent caveolin-3–binding domains, we generated mutated versions of MuSK (mutant A and mutant B) where the aromatic residues were mutated to alanines and cloned the cDNA into the pCMV-HA vector. HA-tagged wild-type MuSK was cloned as a control. The tyrosine residues removed in the mutant MuSK proteins are not residues phosphorylated in MuSK activation (Watty *et al*., 2000). Caveolin-3 was cotransfected with either wild type or one of the mutated forms of MuSK in a heterologous system (Ras^{G12V}-transformed fibroblasts, devoid of caveolin-3 and family member caveolin-1), and their interaction

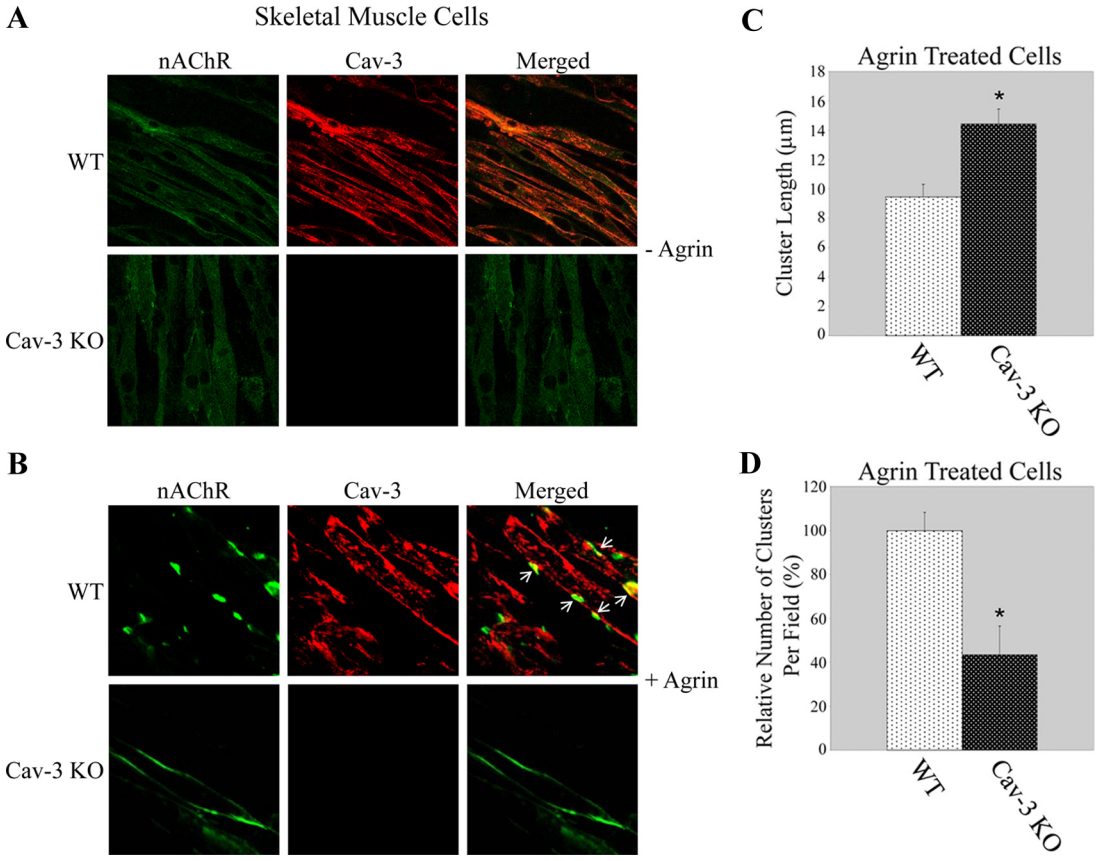

Figure 3. Lack of caveolin-3 alters nAChR clustering. Myogenic precursor cells were derived from wild-type and caveolin-3 null mice, differentiated for 7 d, and treated with and without agrin (10 ng/ml) for 24 h. Cells were stained for nAChR-α (green) and Cav-3 (red) and analyzed by confocal microscopy. Representative images are shown in A (− Agrin) and (B) (+ Agrin). Arrows in B indicate discrete areas of the sarcolemma where nAChR-α and caveolin-3 are enriched. (C) Quantification of cluster length. Values represent means ± SEM, *p = 0.0029. (D) Quantification of the number of clusters per field. Values represent means ± SEM, *p = 0.025.

was examined by coimmunoprecipitation studies. We demonstrate in Figure 4A that wild-type MuSK coimmunoprecipitated with caveolin-3. Coimmunoprecipitation of caveolin-3 with MuSK Mut A was greatly reduced, and it was not detectable with MuSK Mut B. We conclude that caveolin-3 is a novel MuSK-binding protein and amino acids 785-792 and 795-802 of MuSK represent caveolin-3 binding domains.

Lack of Caveolin-3 Prevents Agrin-induced Activation of MuSK

MuSK autophosphorylates upon agrin binding; therefore, tyrosine phosphorylation of MuSK is an indication of its activation. Because we demonstrated that caveolin-3 is a MuSK-binding protein (Figure 4A), we asked whether caveolin-3 expression was required for MuSK phosphorylation/activation. Wild-type and caveolin-3 null myotubes were treated with agrin for different times (15 min, 1 and 4 h). Untreated cells were used as controls. Cell lysates were immunoprecipitated with an antibody probe specific for MuSK, and immunoprecipitates were subjected to immunoblotting analysis by using anti-phosphotyrosine IgGs. We demonstrate in Figure 4B that agrin activation of MuSK in wild-type myotubes peaked after treatment with agrin for 1 h. In contrast, MuSK activation by agrin was dramatically compromised in the absence of caveolin-3 (Figure 4B). Interestingly, we found that agrin promoted the interaction between caveolin-3 and MuSK, with maximal interaction after treatment with agrin for 1 h (Figure 4B). This temporally matched MuSK activation. These results suggest that movement of MuSK to caveolae, where MuSK interacts with caveolin-3, is required for its activation and that lack of MuSK activation in caveolin-3 null myotubes may explain the altered nAChR clustering observed in these cells. Finally, we ruled out that inhibition of nAChR clustering is due to reduced activation of the c-Jun NH_2-terminal kinase (JNK) (Figure 4B), which has also been implicated as a downstream target of agrin treatment (Schaeffer *et al*., 2001).

Lack of Caveolin-3 Inhibits Agrin-induced Activation of Rac1

Rac1 activation has been implicated as a required intermediate step for nAChR clustering in skeletal muscle cells downstream of MuSK (Weston *et al*., 2000, 2003). To further support our hypothesis that impaired nAChR clustering in caveolin-3 null cells is the consequence of reduced MuSK activation, we examined agrin-induced activation of Rac1 in our system. Wild-type and caveolin-3 null myotubes were treated with agrin for 15 min, 1 h, or 4 h. Untreated cells were used as controls. Cells were collected, and activation of Rac1 was determined by GST-PBD pulldowns. Figure 4C shows that agrin promoted Rac1 activation in wild-type but not caveolin-3 null myotubes. Total Rac1 expression was comparable between wild-type and caveolin-3 null cells (Figure 4C). Similar to Rac1 activation, the interaction between

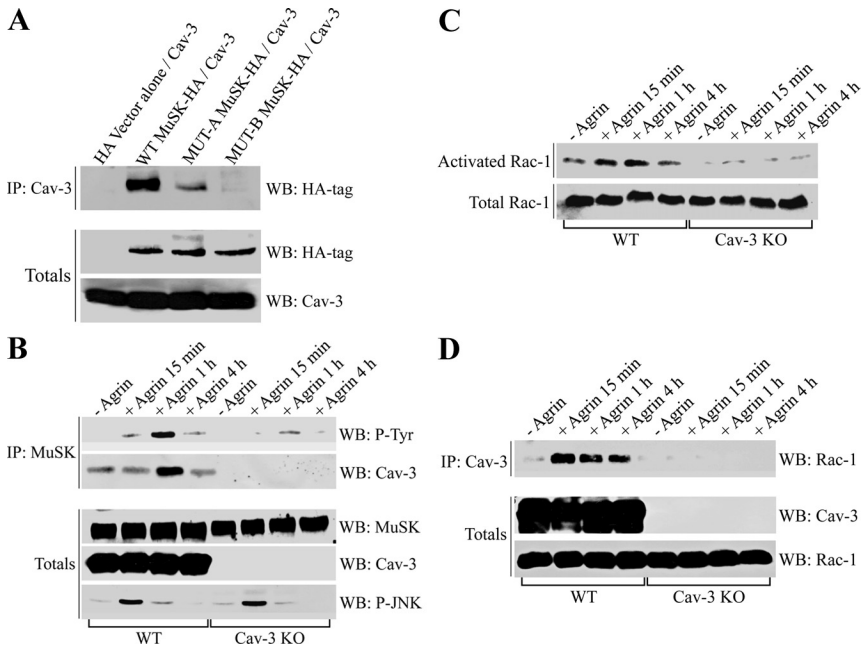

Figure 4. Caveolin-3 expression promotes activation of MuSK and Rac-1 after agrin treatment. (A) Ras^{G12V}-transformed 3T3 cells were transiently cotransfected with caveolin-3 and each of the following constructs: pCMV-HA, pCMV-WT-MuSK-HA, pCMV-mutant A-MuSK-HA, and pCMV-mutant B-MuSK-HA. Forty eight hours after transfection, cell lysates were immunoprecipitated with an antibody probe specific for caveolin-3, and immunoprecipitates were subjected to immunoblotting analysis using anti-HA IgGs. Total expression of Cav-3 and HA-tag–expressing constructs are shown in the two bottom panels. (B–D) Myogenic precursor cells were derived from wild-type and caveolin-3 null mice, differentiated for 7 d, and treated with agrin (10 ng/ml) for 15 min, 1 h, or 4 h. Untreated cells were used as controls. (B) Cell lysates were immunoprecipitated using an antibody probe specific for MuSK, and immunoprecipitates were subjected to immunoblotting analysis using either anti-phosphotyrosine (P-Tyr) or anti-caveolin-3 IgGs. Total MuSK, caveolin-3, and phosphorylated JNK expression are shown in the bottom panel. (C) Cell lysates were immunoprecipitated using GST fused to the PBD of Pak1, and immunoprecipitates were subjected to immunoblotting analysis using anti-Rac-1 IgGs. Total Rac-1 expression is shown in the bottom panel. (D) Cell lysates were immunoprecipitated using an antibody probe specific for caveolin-3, and immunoprecipitates were subjected to immunoblotting using anti-Rac-1 IgGs. Total caveolin-3 and Rac-1 expression are shown in the bottom panel.

caveolin-3 and Rac1 was induced by agrin in wild-type myotubes (Figure 4D), suggesting that lack of interaction between caveolin-3 and Rac1 in caveolin-3 null myotubes may explain lack of Rac1 activation in these cells. Interestingly, comparable dynamics was observed for the interaction between caveolin-3 and MuSK (Figure 4B), activation of MuSK (Figure 4B), and activation of Rac1 (Figure 4C) in wild-type myotubes. Thus, we propose a model where the agrin-induced movement of MuSK to caveolae promotes the activation of a MuSK/Rac1-dependent pathway that leads to clustering of the nAChR (see Figure 7).

Caveolin-3 Expression Is Required for Normal Neuromuscular Junction Activity In Vivo

Because our data show that clustering of the nAChR at the neuromuscular junction is altered in the absence of caveolin-3, one would expect abnormal neuromuscular junction activity in vivo. To directly test this possibility, we performed EMG studies on the gastrocnemius muscle during supramaximal electrical stimulation of the sciatic nerve in wild-type and caveolin-3 null mice. Latency, peak-to-peak amplitude, and area under the curve of the compound muscle action potentials (M response) were measured. We found a longer latency and a smaller amplitude and area under the curve in caveolin-3 null muscle, compared with wild-type muscle (Figure 5, A–C, and Table 1). In addition, there was a wider range in the EMG individual values in caveolin-3 null mice (Figure 5, A–C).

The patterns of muscle contractions evoked by continuous 20-s duration 50-Hz stimulations of the sciatic nerve were also different in the two groups of animals. In wild-type mice, the stimulation elicited a contraction that reached a

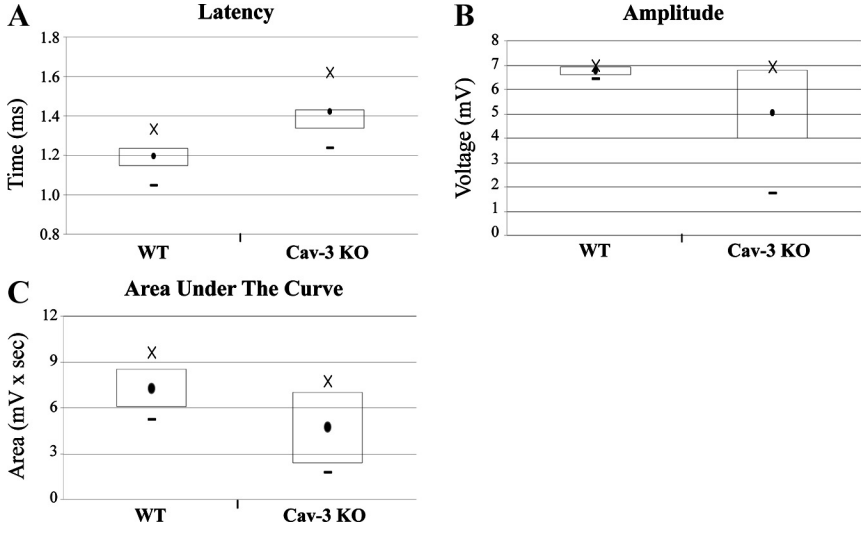

Figure 5. Electromyography analysis in caveolin-3 null mice. Electromyography was performed on gastrocnemius muscle from wild-type and caveolin-3 null mice after nerve stimulation at 10 V/1 Hz. Box-and-whisker plots of the M response latency (A), amplitude (B), and area under the curve (C) are shown. Boxes indicate the middle 50% of the values; dots indicate the average; crosses indicate the highest value; and lines indicate the lowest value. p values, 0.0001 (A), 0.0004 (B), and 0.001 (C).

Table 1. Electromyography studies on wild-type (WT) and caveolin-3 null (Cav-3 KO) mice

Genotype	Latency (ms)	Amplitude (mV)	AUC (mV x sec)
WT	1.1 ± 0.016	6.7 ± 0.029	7.2 ± 0.32
Cav-3 KO	1.4 ± 0.014*	5.0 ± 0.44*	4.6 ± 0.39*
*p value	0.0001	0.0004	0.0001

peak within 1 s, maintains a plateau for 3–6 s and then slowly declined. The responses were relatively smooth tetanic contractions with superimposed small-amplitude 50-Hz phasic contractions (Figure 6). However, in caveolin-3 null mice, the responses were initially biphasic eliciting an initial peak within 2 s and a second peak 4–8 s after the start of stimulation. In addition, large-amplitude phasic contractions (50 Hz) were superimposed on the tonic contraction (Figure 6, A and C). The area of the curve of the phasic contractions was significantly larger in caveolin-3 null versus wild-type mice (Figure 6B).

DISCUSSION

In this study, we analyzed the role of caveolin-3 in nAChR clustering. We found that caveolin-3 expression promoted proper clustering of the nAChR in wild-type myotubes. In contrast, we found a more diffused localization of the nAChR in myotubes lacking caveolin-3. What is the molecular mechanism underlying the altered clustering of the nAChR in caveolin-3 null myotubes? We identified caveolin-3 as a novel MuSK-binding protein and show that a lack of caveolin-3 severely decreases agrin-induced autophosphorylation/activation of MuSK and the consequent activation of Rac-1. Given the key role of MuSK as a mediator of nAChR clustering (DeChiara *et al*., 1996), we conclude that caveolin-3 expression regulates clustering of the nAChR through activation of MuSK/Rac-1 signaling. This is consistent with the positive role that caveolin-3 plays in the activation of the signaling modulated by the insulin receptor, another receptor tyrosine kinase (Yamamoto *et al*., 1998; Fecchi *et al*., 2006). Interestingly, MuSK and the insulin receptor share a conserved caveolin binding domain within their kinase domain (Supplemental Figure 2B). Thus, caveolin-3 acts as a positive regulator of both MuSK and the insulin receptor, and the specificity of its action may depend upon colocalization between caveolin-3 and either MuSK or the insulin receptor within the same cellular microdomain.

Our finding that JNK activation upon agrin treatment is not altered in caveolin-3 null mice, where agrin-induced Rac-1 activation is defective, is in contrast with a previous report showing that agrin-induced JNK phosphorylation was dependent on Rac activation, as shown by lack of c-Jun phosphorylation after transient cotransfection of JNK and dominant-negative Rac-1 in muscle cells (Weston *et al*., 2000). One possible explanation for this discrepancy is the different model system and/or experimental approach used in the two studies, i.e., transient overexpression of JNK in immortalized C2C12 cell line versus endogenous JNK in conditionally immortalized primary cultures used in our study. Alternatively, there may be a compensatory mechanism in caveolin-3 null myotubes that compensates for a lack of Rac-1 activation, such as one modulated by dishevelled (Dvl), as JNK has been shown to be activated by Dvl in a heterologous system (Boutros *et al*., 1998). Nevertheless, normal activation of JNK by agrin in caveolin-3 null cells where clustering of the nAChR is inhibited is consistent with data showing that JNK is not involved in nAChR clustering in muscle cells (Luo *et al*., 2002).

Our data also show that caveolin-3 colocalizes with the nAChR both in muscle fibers in vivo and differentiated myotubes in cell culture studies and that agrin promotes the interaction between caveolin-3 and the nAChR. Interest-

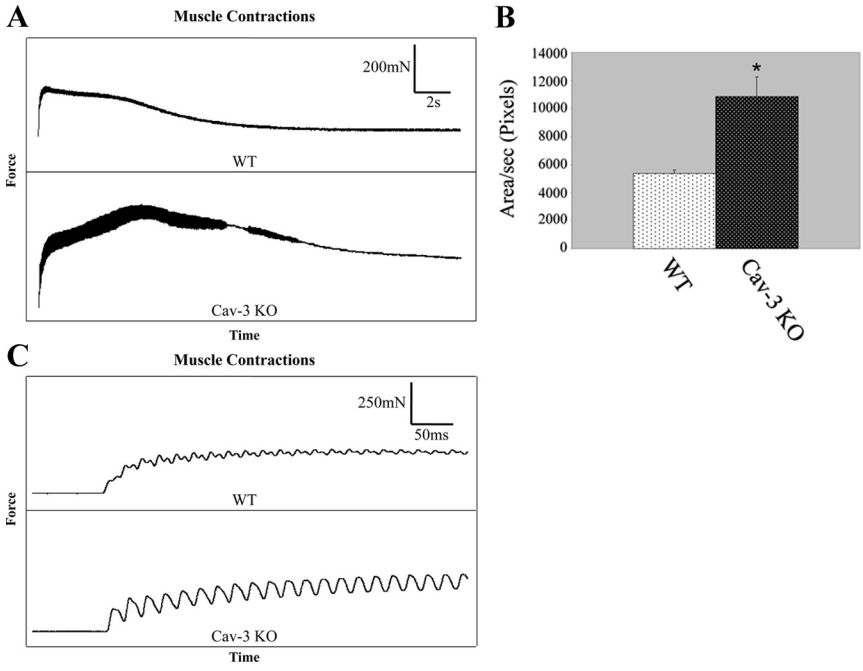

Figure 6. Muscle contraction measurements in wild-type and caveolin-3 null mice. Contractions of gastrocnemius muscle from wild-type and caveolin-3 null mice were recorded during repetitive sciatic nerve stimulation at high frequency (100 V/50 Hz). A representative recording is shown in A. (B) Quantification of the variability of force of muscle contraction after repetitive nerve stimulation was determined by measuring the average traces area per second. Values represent means ± SEM, *p = 0.0034. A representative recording during the first 500 ms is shown in C.

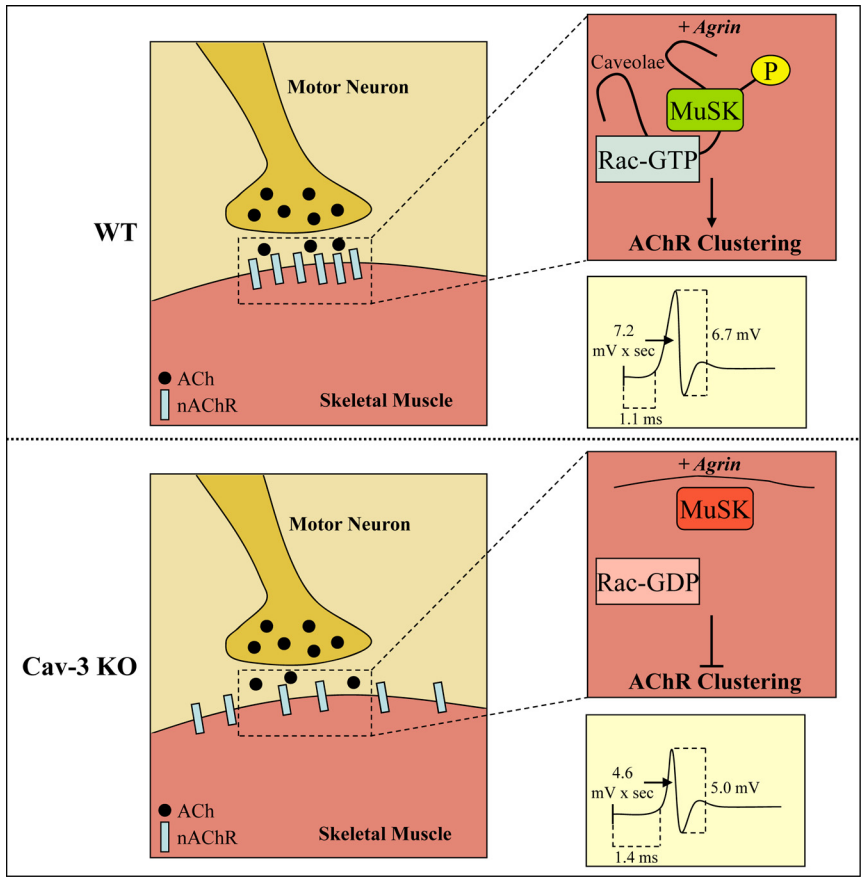

Figure 7. Schematic diagram summarizing the role of caveolin-3 at the neuromuscular junction. In wild-type muscles, caveolin-3 expression allows agrin-induced phosphorylation/activation of MuSK (P-MuSK), activation of Rac-1 (Rac-GTP), and clustering of the nAChR (blue bars). Normal neuromuscular junction activity is recorded by electromyography. In caveolin-3 null muscles, a lack of caveolin-3 prevents the agrin-induced activation of the MuSK/Rac-1 pathway, and the nAChR seems diffusely distributed at the sarcolemma. Abnormal neuromuscular junction activity is recorded by electromyography. ACh, acetylcholine.

ingly, the α subunit of the nAChR has a putative caveolin-binding motif (aa 245–254). We do not know, at this time, whether the interaction between caveolin-3 and the nAChR occurs in a direct or indirect manner. However, because caveolin-3 has been shown to directly interact with proteins carrying a caveolin binding motif and we show in Figure 2C that caveolin-3 and the nAChR interact when coexpressed in a heterologous system, we speculate that caveolin-3 may directly interact with the nAChR in skeletal muscle cells. Because caveolin-3 acts as a scaffolding protein that concentrates and functionally regulates signaling molecules (Couet *et al*., 1997a; Song *et al*., 1997; Okamoto *et al*., 1998), it is possible that caveolin-3 promotes clustering of the nAChR not only by activating MuSK/Rac-1–dependent signaling but also by concentrating the nAChR at the neuromuscular junction through its scaffolding properties after the MuSK/Rac-1–dependent signaling has been activated in a caveolin-3–dependent manner. One may envision a scenario where a subpopulation of caveolin-3 promotes the activation of MuSK, whereas a different pool of caveolin-3 regulates clustering of the nAChR. Alternatively, given that caveolin-3 oligomerizes to form large complexes, the resulting macromolecular structure may provide a platform for both the initial MuSK activation and the consequent nAChR clustering.

Clustering of the nAChR in caveolin-3 null myotubes is, however, not fully abrogated. This may be explained by the notion that other signaling molecules have been shown to contribute to nAChR clustering independently of the MusK/Rac-1 pathway. For example, laminin has been shown to induce clustering through a pathway involving α-dystroglycan (Chockalingam *et al*., 2002; Weston *et al*., 2007). Consistent with this possibility, partial clustering has been shown to still occur in the absence of MuSK activation (Bromann *et al*., 2004).

To identify a functional defect of the neuromuscular junction that may result from an altered caveolin-3/MuSK/Rac-1 signaling, we subjected wild-type and caveolin-3 null mice to EMG studies. We found longer latency and smaller amplitude and area under the curve of compound muscle action potentials in caveolin-3 null muscle. In addition, the individual latency, amplitude, and area under the curve values in caveolin-3 null muscle had a large range in variability. We also measured the intensity of muscle contractions during continuous nerve stimulation. Although the overall force of single muscle contraction was not reduced in caveolin-3 null mice (data not shown), the tonic contractions at 50-Hz stimulation exhibited large-amplitude phasic contractions, indicating that tetanus could not be fully achieved in these muscles at this frequency. The inability of caveolin-3 null mice to maintain tetanic contractions could be explained by a defect in neuromuscular transmission and is consistent with a diffuse localization of the nAChR at the neuromuscular junction of these mice. In fact, sodium currents that are generated after binding of acetylcholine to the nAChR can successfully and consistently generate local muscle depolarization and coordinated muscle contractions only if the nAChR is concentrated in discrete areas within the sarcolemma of each muscle fiber. Alternatively, the failure of caveolin-3 null mice to exhibit a complete tetanic contraction at 50-Hz stimulation could be related to postjunctional changes in the muscle.

Lack or reduced expression of caveolin-3 has been implicated in the development of myopathies. More specifically, mutations of caveolin-3 that lead to down-regulation and/or

misfunction of the protein have been associated to the development of limb girdle muscular dystrophy, hyperCKemia, distal myopathy, and rippling muscle disease (Hezel *et al*., 2005). These pathologies are characterized by great heterogeneity, even among family members, with variability in time of onset, severity of muscle defects, and amount of muscle wasting. Because we demonstrate in this study that a lack of caveolin-3 affects clustering of the nAChR and neuromuscular junction activity, we can speculate that defective caveolin-3–dependent signaling at the neuromuscular junction may contribute, in part, to the defects observed in muscle diseases characterized by mutations in the caveolin-3 gene. Because caveolin-3 null mice exhibit signs of mild muscular dystrophy (Galbiati *et al*., 2001), we cannot rule out the possibility that the limited degeneration/regeneration observed in skeletal muscle tissues of these mice may partially contribute to the observed NMJ abnormalities. We propose the caveolin-3/MuSK/Rac-1 cascade as a novel signaling pathway that regulates clustering of the nAChR and normal neuromuscular junction activity (Figure 7) and a potential therapeutic target for the treatment of muscle disorders characterized by defective neuromuscular signaling.

ACKNOWLEDGMENTS

We thank Dr. Daniela Volonte (Department of Pharmacology and Chemical Biology, University of Pittsburgh, Pittsburgh, PA) for providing caveolin-3 null mice, Dr. Zuo-Zhong Wang for advice and suggestions, and Bradley H. Morneweck for help with immunofluorescence studies. This work was supported by National Institutes of Health National Institute on Aging grants R01-AG022548 and R01-AG030636 (to F. G.). M. H. was supported by a National Institutes of Health predoctoral training grant in pharmacological sciences (T32-GM08424).

REFERENCES

Aravamudan, B., Volonte, D., Ramani, R., Gursoy, E., Lisanti, M. P., London, B., and Galbiati, F. (2003). Transgenic overexpression of caveolin-3 in the heart induces a cardiomyopathic phenotype. Hum. Mol. Genet. *12*, 2777–2788.

Boutros, M., Paricio, N., Strutt, D. I., and Mlodzik, M. (1998). Dishevelled activates JNK and discriminates between JNK pathways in planar polarity and wingless signaling. Cell *94*, 109–118.

Bromann, P. A., Zhou, H., and Sanes, J. R. (2004). Kinase- and rapsyn-independent activities of the muscle-specific kinase (MuSK). Neuroscience *125*, 417–426.

Chockalingam, P. S., Cholera, R., Oak, S. A., Zheng, Y., Jarrett, H. W., and Thomason, D. B. (2002). Dystrophin-glycoprotein complex and Ras and Rho GTPase signaling are altered in muscle atrophy. Am. J. Physiol. Cell Physiol. *283*, C500–C511.

Couet, J., Li, S., Okamoto, T., Scherer, P. S., and Lisanti, M. P. (1997a). Molecular and cellular biology of caveolae: paradoxes and plasticities. Trends Cardiovasc. Med. *7*, 103–110.

Couet, J., Li., S., Okamoto, T., Ikezu, T., and Lisanti, M. P. (1997b). Identification of peptide and protein ligands for the caveolin-scaffolding domain. Implications for the interaction of caveolin with caveolae-associated proteins. J. Biol. Chem. *272*, 6525–6533.

DeChiara, T. M., *et al*. (1996). The receptor tyrosine kinase MuSK is required for neuromuscular junction formation in vivo. Cell *85*, 501–512.

Fecchi, K., Volonte, D., Hezel, M. P., Schmeck, K., and Galbiati, F. (2006). Spatial and temporal regulation of GLUT4 translocation by flotillin-1 and caveolin-3 in skeletal muscle cells. FASEB J. *20*, 705–707.

Ferns, M. J., Campanelli, J. T., Hoch, W., Scheller, R. H., and Hall, Z. (1993). The ability of agrin to cluster AChRs depends on alternative splicing and on cell surface proteoglycans. Neuron *11*, 491–502.

Galbiati, F., Engelman, J. A., Volonte, D., Zhang, X. L., Minetti, C., Li, M., Hou, H., Jr., Kneitz, B., Edelmann, W., and Lisanti, M. P. (2001). Caveolin-3 null mice show a loss of caveolae, changes in the microdomain distribution of the dystrophin-glycoprotein complex, and t-tubule abnormalities. J. Biol. Chem. *276*, 21425–21433.

Hagiwara, Y., Nishina, Y., Yorifuji, H., and Kikuchi, T. (2002). Immunolocalization of caveolin-1 and caveolin-3 in monkey skeletal, cardiac and uterine smooth muscles. Cell Struct. Funct. *27*, 375–382.

Hezel, M. P., Bartholomew, J. N., and Galbiati, F. (2005). Caveolin-3, its importance in muscle function and pathology. Curr. Genomics *6*, 293–314.

Li, S., Galbiati, F., Volonte, D., Sargiacomo, M., Engelman, J. A., Das, K., Scherer, P. E., and Lisanti, M. P. (1998). Mutational analysis of caveolin-induced vesicle formation. Expression of caveolin-1 recruits caveolin-2 to caveolae membranes. FEBS Lett. *434*, 127–134.

Luo, Z. G., Wang, Q., Zhou, J. Z., Wang, J., Luo, Z., Liu, M., He, X., Wynshaw-Boris, A., Xiong, W. C., Lu, B., and Mei, L. (2002). Regulation of AChR clustering by Dishevelled interacting with MuSK and PAK1. Neuron *35*, 489–505.

Moldovan, N., Heltianu, C., Simionescu, N., and Simionescu, M. (1995). Ultrastructural evidence of differential solubility in Triton X-100 of endothelial vesicles and plasma membrane. Exp. Cell Res. *219*, 309–313.

Okamoto, T., Schlegel, A., Scherer, P. E., and Lisanti, M. P. (1998). Caveolins, A family of scaffolding proteins for organizing "pre-assembled signaling complexes" at the plasma membrane. J. Biol. Chem. *273*, 5419–5422.

Razani, B., Schlegel, A., and Lisanti, M. P. (2000). Caveolin proteins in signaling, oncogenic transformation and muscular dystrophy. J. Cell Sci. *113*, 2103–2109.

Sanes, J. R., and Lichtman, J. W. (2001). Induction, assembly, maturation and maintenance of a postsynaptic apparatus. Nat. Rev. Neurosci. *2*, 791–805.

Schaeffer, L., de Kerchove d'Exaerde, A., and Changeux, J. P. (2001). Targeting transcription to the neuromuscular synapse. Neuron *31*, 15–22.

Song, K. S., Sargiacomo, M., Galbiati, F., Parenti, M., and Lisanti, M. P. (1997). Targeting of a G alpha subunit (G_{i1} alpha) and c-Src tyrosine kinase to caveolae membranes: clarifying the role of N-myristoylation. Cell. Mol. Biol. *43*, 293–303.

Tang, Z.-L., Scherer, P. E., Okamoto, T., Song, K., Chu, C., Kohtz, D. S., Nishimoto, I., Lodish, H. F., and Lisanti, M. P. (1996). Molecular cloning of caveolin-3, a novel member of the caveolin gene family expressed predominantly in muscle. J. Biol. Chem. *271*, 2255–2261.

Volonte, D., McTiernan, C. F., Drab, M., Kasper, M., and Galbiati, F. (2008). Caveolin-1 and caveolin-3 form heterooligomeric complexes in atrial cardiac myocytes that are required for doxorubicin-induced apoptosis. Am. J. Physiol. Heart Circ. Physiol. *294*, H392–H401.

Volonte, D., Peoples, A. J., and Galbiati, F. (2003). Modulation of myoblast fusion by caveolin-3 in dystrophic skeletal muscle cells: implications for Duchenne muscular dystrophy and limb-girdle muscular dystrophy-1C. Mol. Biol. Cell *14*, 4075–4088.

Watty, A., Neubauer, G., Dreger, M., Zimmer, M., Wilm, M., and Burden, S. J. (2000). The in vitro and in vivo phosphotyrosine map of activated MuSK. Proc. Natl. Acad. Sci. USA *97*, 4585–4590.

Weston, C., Gordon, C., Teressa, G., Hod, E., Ren, X. D., and Prives, J. (2003). Cooperative regulation by Rac and Rho of agrin-induced acetylcholine receptor clustering in muscle cells. J. Biol. Chem. *278*, 6450–6455.

Weston, C., Yee, B., Hod, E., and Prives, J. (2000). Agrin-induced acetylcholine receptor clustering is mediated by the small guanosine triphosphatases Rac and Cdc42. J. Cell Biol. *150*, 205–212.

Weston, C. A., Teressa, G., Weeks, B. S., and Prives, J. (2007). Agrin and laminin induce acetylcholine receptor clustering by convergent, Rho GTPase-dependent signaling pathways. J. Cell Sci. *120*, 868–875.

Williams, T. M., and Lisanti, M. P. (2004). The Caveolin genes: from cell biology to medicine. Ann. Med. *36*, 584–595.

Yamamoto, M., Toya, Y., Schwencke, C., Lisanti, M. P., Myers, M., and Ishikawa, Y. (1998). Caveolin is an activator of insulin receptor signaling. J. Biol. Chem. *273*, 26962–26968.